

# Cloud Computing for Seizure Detection in Implanted Neural Devices

Steven Baldassano<sup>1,2</sup>, Xuelong Zhao<sup>1,2</sup>, Benjamin Brinkmann<sup>3,4</sup>, Vaclav Kremen<sup>3,4,5</sup>, John Bernabei<sup>1,2</sup>, Mark Cook<sup>6,7</sup>, Timothy Denison<sup>8,9</sup>, Gregory Worrell<sup>3,4</sup>, Brian Litt<sup>1,2,10</sup>

<sup>1</sup>Department of Bioengineering, University of Pennsylvania, Philadelphia, PA 19104, USA

<sup>2</sup>Center for Neuroengineering and Therapeutics, University of Pennsylvania, Philadelphia, PA 19104, USA

<sup>3</sup>Mayo Systems Electrophysiology Laboratory, Department of Neurology, Mayo Clinic, Rochester, MN, USA

<sup>4</sup>Department of Physiology and Biomedical Engineering, Mayo Clinic, Rochester, MN, USA

<sup>5</sup>Czech Institute of Informatics, Robotics and Cybernetics, Czech Technical University in Prague, Czech Republic

<sup>6</sup>St. Vincent's Hospital, Melbourne, VIC, Australia

<sup>7</sup>Department of Medicine, University of Melbourne, Melbourne, VIC, Australia

<sup>8</sup>Department of Engineering Science, University of Oxford, Oxford UK

<sup>9</sup>Research and Technology, Restorative Therapy Group, Medtronic, Minneapolis, MN, USA

<sup>10</sup>Department of Neurology, University of Pennsylvania, PA, USA

## Abstract

**Objective:** Closed-loop implantable neural stimulators are an exciting treatment option for patients with medically refractory epilepsy, with a number of new devices in or nearing clinical trials. These devices must accurately detect a variety of seizure types in order to reliably deliver therapeutic stimulation. While effective, broadly-applicable seizure detection algorithms have recently been published, these methods are too computationally intensive to be directly deployed in an implantable device. We demonstrate a strategy that couples devices to cloud computing resources in order to implement complex seizure detection methods on an implantable device platform.

**Approach:** We use a sensitive gating algorithm capable of running on-board a device to identify potential seizure epochs and transmit these epochs to a cloud-based analysis platform. A precise seizure detection algorithm is then applied to the candidate epochs, leveraging cloud computing resources for accurate seizure event detection. This seizure detection strategy was developed and tested on eleven human implanted device recordings generated using the NeuroVista Seizure Advisory System.

**Main Results:** The gating algorithm achieved high-sensitivity detection using a small feature set as input to a linear classifier, compatible with the computational capability of next-generation implantable devices. The cloud-based precision algorithm successfully identified all seizures transmitted by the gating algorithm while significantly reducing the false positive rate. Across all subjects, this joint approach detected 99% of seizures with a false positive rate of 0.03/hr.

**Significance:** We present a novel framework for implementing computationally intensive algorithms on human data recorded from an implanted device. By using telemetry to intelligently access cloud-based computational resources, the next generation of neuro-implantable devices will leverage sophisticated algorithms with potential to greatly improve device performance and patient outcomes.

## **Introduction**

Implanted devices are increasingly employed to treat a wide variety of medical conditions, including orthopedic, cardiac, and neurological disorders<sup>1</sup>. Many of these devices, such as implanted pacemakers and defibrillators, drug delivery systems, neural stimulators, and prosthetics, use closed-loop technology to monitor physiologic parameters and delivery therapy<sup>2,3</sup>. In epilepsy, these devices are now entering mainstream clinical care for patients who do not respond to antiseizure medications.

Neural stimulators for treating epilepsy are providing encouraging clinical results<sup>4,5</sup> as our experience with closed-loop implantable devices increases<sup>6</sup>. The FDA approved the first such device, the NeuroPace RNS system, in 2013. This device monitors the intracranial electroencephalogram (iEEG) from depth or subdural electrodes. Seizure detection algorithms identify potential seizure epochs, and electrical stimulation is delivered to arrest seizure evolution and propagation<sup>7</sup>. Responsive stimulation of the anterior nucleus of the thalamus<sup>8</sup>, seizure generators in the cerebral cortex<sup>9</sup>, and hippocampus<sup>10,11</sup> has been demonstrated to effectively decrease clinical seizure frequency, with recent studies reporting up to 72% reduction in seizures, on average<sup>12</sup>. These devices offer an additional treatment option for the 33% of patients with epilepsy who continue to have seizures despite medical and surgical therapy.<sup>13,4</sup> These implanted devices also generate a catalogue of continuous iEEG activity for seizure diaries, providing key information for tracking seizure frequency and guiding medical therapy.

Effective responsive neurostimulation, like other closed-loop therapies, requires highly accurate algorithms to classify brain signals<sup>14–17</sup>. Many machine learning algorithms have been reported to identify seizure activity from EEG<sup>18</sup>, but these results were not easily validated because there was no means for openly sharing data, algorithms, and expert

annotations. Recently, our group led international, crowd-sourced efforts to produce highly accurate, open-source algorithms that robustly detected and forecasted seizures in a large corpus of canine and human implanted device recordings<sup>7,19</sup>. While the performance of these algorithms is impressive, it is not straightforward to implement seizure detection or forecasting algorithms in an implanted device. Such algorithms typically rely on hundreds of signal characteristics such as spectrographic and cross-channel correlational features, which serve as inputs to complex classifiers such as random forests or neural networks. In addition, it is often necessary to pre-process incoming data in one or several filtering steps. Despite improvements in technology miniaturization and power management, the local computational resources of implanted neuroresponsive devices are limited. For example, the on-board processing abilities of both the NeuroPace RNS system and second-generation closed-loop devices currently in development<sup>20</sup> limit analysis to a few simple signal features. The NeuroPace RNS device relies on signal line length<sup>21</sup>, area, and halfwave<sup>22</sup> features to detect seizures using empirically determined feature thresholds<sup>23</sup> that are iteratively adapted to individual patients through repeated office visits over time. More recent devices, such as Medtronic's Activa PC+S implant<sup>24,25</sup>, are capable of computing several bandpower features and applying simple classifiers such as linear discriminant analysis (LDA)<sup>26</sup>. In addition to processing power restrictions, these devices are limited by battery life. Batteries are still large in comparison to microfabricated components<sup>2</sup>, and must power both the computational and stimulation circuitry in the device. While some devices allow for wireless battery recharging, the battery power of existing devices is not sufficient to support continuous seizure detection classifiers. Because detection systems must identify seizure events early and with high sensitivity

while operating within the hardware capabilities of these devices, they suffer from high rates of false detections and, in some implementations, stimulations.<sup>3</sup> Recent research suggests that these frequent stimulations may actually be important to the neuromodulatory effects of these devices<sup>27–29</sup>. This ongoing work has led to parallel approaches in neuromodulation for epilepsy: regular, intermittent, open-loop stimulation to suppress seizures, or responsive, closed-loop stimulation to preempt seizures when they begin or when predictive algorithms indicate high probability of seizure onset<sup>30</sup>.

One approach for applying complex algorithms to implanted device data is to transmit data from the device to a remote platform for analysis. Integrated telemetry for implanted devices has improved significantly over the past decade<sup>31–33</sup>, and is a feature of neuroresponsive devices currently in development<sup>34,35</sup>. However, most state-of-the-art devices are unable to provide sufficient battery power for continuous telemetry, and are limited to streaming four channels of iEEG data for about eight hours before needing to be recharged. It remains a challenge to accurately detect seizures and guide stimulation 24 hours per day while operating within these constraints.

We present a paradigm for implementing a complex seizure detection algorithm on implanted device iEEG data from human subjects. This framework uses a gating algorithm capable of running on-board the implantable to control selective communication between the device and a cloud-based analysis platform for up-front data reduction. The transmitted data is remotely analyzed by a precise seizure detection algorithm that leverages cloud-based computational resources for accurate seizure event detection. We validate this approach in a series of pseudoprospective experiments using pre-recorded, continuous

human data. Finally, we discuss ongoing efforts, and remaining barriers, toward implementing this novel approach in routine clinical care.

## **Methods**

### *Subjects and Data*

In order to mimic the target application of implanted device recordings, the system was developed and evaluated using eleven continuous human intracranial EEG datasets generated from the NeuroVista Seizure Advisory System described previously<sup>36</sup>. Intracranial EEG was acquired from the device with a sampling rate of 400Hz from 16 subdural electrodes arranged on four standard, human-sized, 4-contact strips. EEG data was lowpass filtered at 180Hz using a third order Butterworth filter. Strips were placed according to individual clinical considerations to target the seizure onset location. Patients were recorded for up to 2 years with continuous intracranial EEG via an implanted telemetry device coupled to a belt-worn unit<sup>36</sup>. All seizure start times were annotated by board certified epileptologists (G.W., B.L., M.C.). Seizure start was defined as the time of earliest electrographic change (EEC), the earliest point at which an epileptologist with knowledge of ensuing seizures is able to discern a change from background<sup>37</sup>. More details and metadata regarding these datasets can be found in Supplemental Figure 1 and Supplemental Tables 1 and 2.

### *Detection Paradigm*

Seizure detection was carried out using a novel paradigm to leverage cloud-computing resources. In this scheme, two detection algorithms are sequentially applied to the data. The first algorithm, termed the “gating algorithm,” is a hypersensitive detector using only a few (up to five) simple signal features. This detector is designed to be compatible with the computational limitations of an implanted device, such the NeuroPace

RNS or Medtronic Activa RC+S.

Potential seizure epochs identified by the gating algorithm are selectively transmitted from the device to a cloud-based data system. These clips are then analyzed by the second algorithm, termed the “precision algorithm,” which provides highly accurate

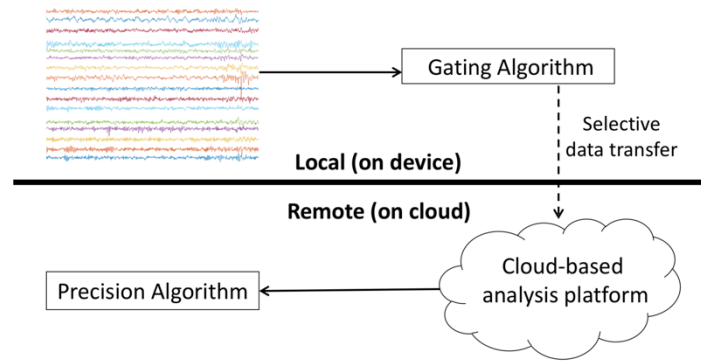


**Figure 1.** Seizure detection paradigm using cloud computing. Potential seizure clips are identified using a hypersensitive, on-board seizure detector. These clips are transmitted to a cloud platform for analysis using a highly accurate, computationally intensive algorithm.

but computationally intensive seizure detection. This algorithm was the winner of an open seizure detection competition hosted on kaggle.com<sup>7</sup>. The precision algorithm was implemented using cloud resources to provide final seizure detections. This detection paradigm is shown in Figure 1. While ongoing work has confirmed the feasibility of applying such a system *in vivo* (see Discussion), it is important to note that our experiments relied on offline recorded datasets rather than true real-time recordings. “On-board” computation was carried out using a 2014 Macbook Pro (2.5GHz Intel Core i7, 16GB memory), and cloud computation was carried out on a remote server (Rackform R331.v5 server with 32 Intel Xeon E5-2698v3 (2.3GHz) cores and 256GB memory).

### *Detection algorithms*

- 1) Gating algorithm – The gating algorithm is required to identify potential seizure clips (while accepting a high level of false positives) with very little processing power at runtime. For this purpose, we used a logistic regression classifier trained on up to five signal features. These features are empirically chosen on a per-patient

basis during training from a single manually-constructed feature bank containing bandpower features (Welch's power spectral density computed in 25 manually-chosen, partially-overlapping frequency bands of varying length covering the range from 5 to 70 Hz for each channel), cross-correlation features (normalized cross-correlation of each pairwise combination of channel signals<sup>38,39</sup> with 0.05s of lag), and line length features<sup>21</sup> (computed for each channel as the sum of the magnitude of the first signal derivative over time). Further details regarding feature computation are found in Supplemental Methods. Feature sets were selected from this bank using a greedy stepwise process<sup>40</sup> to add one feature at a time, choosing the feature at each step that provides the lowest misclassification error on cross validation. All cross validation and feature selection was carried out using training data only. The computer used to run the gating algorithm in this analysis is not representative of an implanted chip's processing power, so care was taken to ensure compatibility of the algorithm with an implanted device. This was done by two methods: (1) the gating algorithm (including feature types, number of features, and classifier type) was designed in collaboration with Medtronic engineers to ensure compatibility with the known capabilities of implantable device hardware and computational resources, and (2) a version of this algorithm using the same feature types, feature number, and classifier type was successfully implemented in the Activa RC+S device as a proof of concept.<sup>35</sup>

- 2) Precision algorithm – The precision algorithm has been described in detail in Baldassano, et al., 2017<sup>7</sup>. This algorithm relies on three sets of features for

classification, which are extracted from one-second, non-overlapping segments of iEEG data. The first set of features consists of the pairwise cross-correlation between channel signals as well as the sorted eigenvalues of the cross-correlation matrix. A Fast Fourier Transform (FFT) is then applied to the data to generate a frequency domain representation. The second set of features consists of the frequency magnitudes of each channel in the range of 1-47 Hz. This empirically-determined spectrum covers the frequency range typically associated with epileptic events<sup>41-43</sup>; inclusion of higher frequencies to capture high-frequency oscillations (HFOs)<sup>44</sup> did not improve performance. These power spectra are then normalized within each frequency bin. The third set of features consists of the pairwise cross-correlation between normalized channel power spectra in the range of 1-47Hz as well as the sorted eigenvalues of the cross-correlation matrix. A random forest classifier of 3000 trees is trained on the union of the three feature sets.

### *Training and evaluation*

In order to properly implement a simulated prospective study, both the gating and precision algorithms were trained on a per-patient basis in order to capture subject-specific seizure morphology. The training, validation, and testing datasets were drawn from chronologically distinct (non-overlapping) segments of EEG from each individual patient. Training data included up to 20 seizures per patient selected chronologically from the start of the recording, using at least 6 seizures per patient to ensure an adequate number of training observations<sup>7</sup> (more detail can be found in Supplemental Table 1.) Training seizures were selected to include all seizures spanning several months after implantation in order to avoid transient changes in signal features characteristic of the post-implantation



state<sup>45</sup>. Both detection algorithms were trained on unbalanced datasets, with the number of interictal data clips outnumbering the number of ictal data clips. During gating algorithm tuning, the loss associated with misclassifying an interictal clip was set to unity while the loss associated with misclassifying an ictal clip was set to the ratio in the number of interictal to ictal clips. This approach was intended to increase the sensitivity of the classifier.

The performance of the gating detector was evaluated for each subject using validation data consisting of up to 20 seizures (Supplemental Table 1), which occurred chronologically following the training data. These validation data were used to assess the impact of varying the number of features (ranging from 1 to 5) and including different feature types (bandpower features vs. cross-correlation features vs. line length features) on algorithm performance. In these preliminary tuning trials, performance was assessed by the area under a receiver operating characteristic (ROC) curve for the classification of one-second clips as seizure or non-seizure activity.

The full detection system (incorporating the tuned gating algorithm) was then evaluated on the remainder of the data held out as a test set. While we rely on offline data, these recordings were evaluated chronologically such that the model has no knowledge of future events in order to simulate a prospective use case. Seizure detections were post-processed using a convolutional filter to sum the seizure likelihoods of each one-second clip within a moving window. A five-second window was used for the gating algorithm and a two-second window was used for the precision algorithm. A detection was generated if this sum exceeded an empirical threshold, indicating high likelihood of sustained seizure activity. This approach decreased false positive detections and allowed for sensitivity

titration by adjusting the detection threshold. Evaluation began six hours after the last training seizure and continued until the end of the recording, incorporating between 2 and 201 seizures per patient (Table 2). The potential seizure clips identified for evaluation by the precision algorithm were not modified or transformed in any way by the gating algorithm.

## **Results**

ROC curves for the gating algorithm are shown in Figure 2. ROC curves were generated using one to five features from either the full feature bank, a bank of just frequency features, or a bank of the frequency and cross-correlation features. The area under each of these ROC curves is shown in Table 1. While classification performance tended to increase with addition of more features, this benefit is negligible in all training scenarios once at least three features have been added. A particularly interesting result is that inclusion of cross-correlation and line length features does not meaningfully increase performance compared to using bandpower features alone, and that only two bandpower features is sufficient to maximize performance in this cohort.

These preliminary trials also reveal the most discriminative features and sets of features for each patient. The distributions of selected feature types for each patient are shown in Supplemental Figure 2. In general, frequency band features were the most useful for classification, accounting for 39 of the 55 chosen features overall. A frequency band feature was chosen as the most discriminative feature in nine of eleven subjects and the second most discriminative feature in eight of eleven subjects. The next most-useful class of features was cross-correlation, comprising 14 of the 55 chosen features; however, a cross-correlation feature was not the most discriminative feature in any subject.

The joint seizure detection system was applied to the entirety of each patient's data. The test data was analyzed chronologically and was not preprocessed or curated in any way. Trials were carried out using 1-feature and 5-feature gating algorithms (with all feature types included in the feature bank), with the same precise algorithm applied in each case. The results of these tests are shown in Tables 2 and 3.

Using the single-feature detector, at least 92% of all seizures in each subject (and 95% overall) were detected and transmitted by the gating algorithm prior to seizure termination. This algorithm reduced the iEEG data by a factor of 24.4 across all patients. The five-feature detector was more sensitive, detecting at least 98% in each patient and 99% overall, with a similar specificity, reducing data transfer by a factor of 22.7. The precise, cloud-based detection algorithm successfully identified all seizures transmitted from the device in all cases with an average false positive rate of 0.03 detections per hour of recording.

The latency associated with algorithm computation was compatible with real-time implementation. The gating algorithm analyzed one hour of recorded data in  $16.5 \pm 0.3$  seconds, and the precision algorithm analyzed one hour of transmitted data in  $17.4 \pm 0.2$  seconds. Together, these algorithms introduce a latency under 10ms if recorded data is analyzed in one-second clips. While our experimental setup does not allow for direct measurement of data transfer time from an implanted device, the raw iEEG data is a low-bandwidth signal of about 40kb per second of recording, well within the streaming capabilities of standard 4G LTE networks<sup>46</sup>.

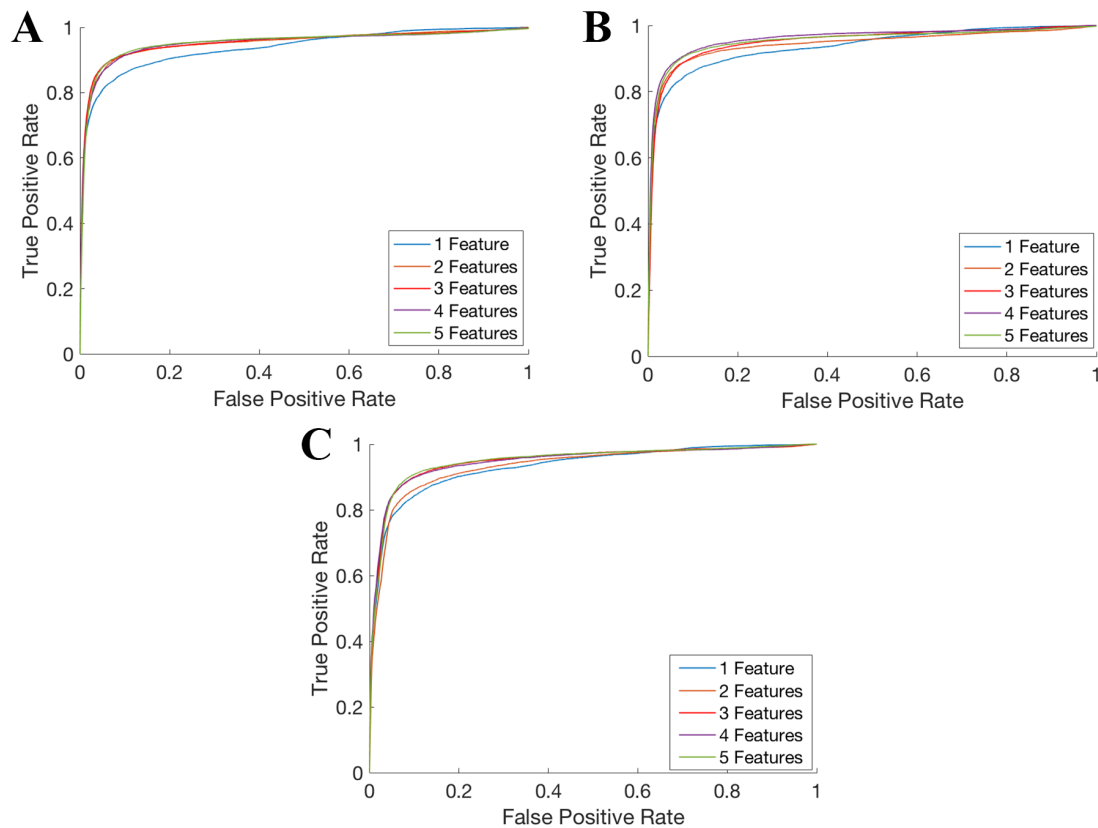


**Figure 2.** ROC curves for the gating algorithm. The gating algorithm was evaluated in an independent test set using **(A)** a bank of bandpower features, **(B)** bandpower and cross-correlation features, or **(C)** bandpower, cross-correlation, and line length features. In each case, the number of features selected was varied from 1 to 5.

<b>Number of Features</b>	<b>Frequency</b>	<b>Frequency and Correlation</b>	<b>Frequency, Correlation, and Line Length</b>
<b>1</b>	0.9369	.9366	.9317
<b>2</b>	0.9516	.9441	.9331
<b>3</b>	0.9526	.9518	.9484
<b>4</b>	0.9517	.9602	.9472
<b>5</b>	0.9531	.9539	.9489

**Table 1.** AUC values for each ROC curve. Performance increases in general as more features are added to the models, but performance plateaus after three features are added. Including cross-correlation and line length features in the feature bank did not improve performance.

	Pt1	Pt2	Pt3	Pt4	Pt5	Pt6	Pt7	Pt8	Pt9	Pt10	Pt11	Avg
<b>Recording length (days)</b>	771	730	558	233	273	117	559	395	374	551	472	458
<b>Data transmitted per 24 hours of recording (hours)</b>	1.13	0.17	0.78	1.41	1.16	0.59	1.31	0.65	0.97	1.02	1.87	1.01
<b>Transmission sensitivity (frac. of seizures)</b>	43/44	11/11	179/188	5/5	2/2	55/60	187/201	147/158	254/265	4/4	44/44	95%
<b>Kaggle detection sensitivity</b>	100%	100%	100%	100%	100%	100%	100%	100%	100%	100%	100%	100%
<b>Joint detection sensitivity</b>	98%	100%	95%	100%	100%	92%	93%	93%	100%	100%	100%	97%
<b>False positive rate per hour</b>	0.04	0.01	0.05	0.05	0.04	0.02	0.04	0.02	0.04	0.02	0.07	0.04

**Table 2.** Results of pseudoprospective analysis using a 1-feature gating algorithm

	Pt1	Pt2	Pt3	Pt4	Pt5	Pt6	Pt7	Pt8	Pt9	Pt10	Pt11	Avg
<b>Recording length (days)</b>	771	730	558	233	273	117	559	395	374	551	472	458
<b>Data transmitted per 24 hours of recording (hours)</b>	1.50	0.064	1.38	1.12	0.80	1.35	1.09	1.65	0.78	0.88	1.43	1.09
<b>Transmission sensitivity (frac. of seizures)</b>	43/44	11/11	184/188	5/5	2/2	60/60	196/201	158/158	261/265	4/4	44/44	99%
<b>Kaggle detection sensitivity</b>	100%	100%	100%	100%	100%	100%	100%	100%	100%	100%	100%	100%
<b>Joint detection sensitivity</b>	98%	100%	98%	100%	100%	100%	98%	100%	98%	100%	100%	99%
<b>False positive rate per hour</b>	0.05	0.01	0.04	0.03	0.02	0.03	0.03	0.07	0.02	0.02	0.03	0.03

**Table 3.** Results of pseudoprospective analysis using a 5-feature gating algorithm

## Discussion

We have shown, using extended implantable device recordings from human subjects, that integrating a highly sensitive gating algorithm and a precise cloud-based algorithm offers more accurate seizure detection than existing neuro-implantable devices, which operate on simple algorithms alone<sup>3</sup>. Current devices, such as the NeuroPace RNS<sup>3</sup>, tolerate a high false positive rate in order to achieve adequate sensitivity, resulting in a high frequency of stimulations on abnormal EEG activity that is not a seizure. In our approach, the high false positive rate of the gating algorithm is mitigated by the precision algorithm, which makes the final decision on streamed data and thus controls the overall false positive rate of the system. By postprocessing algorithm output over multiple-second time scales, we were also able to reduce the false positive rate significantly compared to previous benchmarks<sup>7</sup>. This approach will decrease the number of false positives and provide an accurate seizure diary with high sensitivity and specificity. Furthermore, if high accuracy responsive stimulation on seizures improves clinical efficacy, this method will reduce the amount of unnecessary stimulation that future implantable devices deliver without sacrificing detection sensitivity.

One of the primary goals of this work was to develop an algorithm that is specifically capable of functioning on-board a continuously operational implantable device. For this reason, in the current study we intentionally limited the number and type of features included in the on-board detector with goal of maximizing performance while operating within the processing and battery constraints of such a device. The specific features selected for a given patient were identified in an empiric, data-driven manner from a bank of device-compatible features. Our results suggest that effective on-board seizure detection can be performed using only a small number of features. This finding is encouraging for implementing detectors in low-powered devices as spectral features can



be easily computed using hardware<sup>47,48</sup>, circumventing the need to run a software-based feature extraction algorithm. In the current study, we found that the performance of our on-board detector plateaued after including only 2 or 3 features, well within the limits of feasibility for analog, on-chip processing. The compatibility of this detector with an implanted device is supported by ongoing *in vivo* trials, in which a version of this algorithm has already been successfully implemented in a next-generation implantable neuroresponsive device currently under development at Medtronic, the Activa RC+S neurostimulator<sup>34,35</sup>.

It is important to note that current devices require at least some degree of on-board method implementation. While the newest devices are capable of uploading data to the cloud close to real time<sup>49</sup>, battery life is insufficient for 24/7 data transfer and battery recharging constitutes a nontrivial burden on patients<sup>50</sup>. By gating transmission of data from the device to the cloud, we are able to limit data transmission to only a few hours total per day, significantly reducing energy expenditure. Furthermore, network connections through Wi-Fi or cellular data are not reliable enough for a therapeutic device that must not miss critical event. In the event of network disconnection, the on-board detector could be used therapeutically to ensure a response to all seizures. Technological improvements may someday shift all continuous data analysis entirely to the cloud, but such a system is currently far from practical.

While many seizure detection methods include a pre-processing step, the approach presented in this work represents a unique detection strategy. The particular design of the gating and precision algorithms is unique to this work, as the gating algorithm was designed with deliberate limitation of computational requirements for compatibility with a low-processing-power environment. In addition, the “pre-processing” step on the device solely carries out data reduction and identification of potential seizure clips, rather than data modification or transformation. In

contrast to tradition detection methods employing sequential algorithms, both the gating and precision algorithms analyze the same raw EEG input but in different computational spaces. Finally, this work represents, to our knowledge, the first evaluation of such a system in extended implanted device recordings from human subjects.

There are several limitations of this system to consider. For this framework to be effective in a real-world application, it must not only operate within the hardware specifications of an implanted device, but also work quickly enough to allow for therapeutic intervention<sup>51</sup>. Response latency is primarily governed by (1) algorithm computation time and (2) speed of data transmission to and from the device. While we have shown that algorithm computation introduces only trivial delay, the flow of information between device and cloud was simulated so we were unable to measure transmission-associated latency. These devices produce signals that require very low bandwidth; for instance, the 40kbps requirement for 16-channel iEEG streaming is less than typical data speeds needed for WiFi audio calling. Transmission latency could also be minimized by using a local computational unit, such as a belt-worn pad device or cell phone/PDA, rather than a remote server requiring internet access. Preliminary trials implementing this approach in the Medtronic RC+S device, with off-board computation performed by a local hand-held device<sup>35</sup>, have demonstrated total latency (including data storage, transmission, analysis, and delivery of stimulation) under 200ms. Further *in vivo* testing must be carried out in order to assess the clinical relevance of this response latency.

In over 120,000 hours of data analyzed in our study, 14 of 982 clinically observed seizures were undetected by the gating algorithm. Each undetected seizure was manually reviewed. While some seizures were missed by the 1-feature detector due to variations in seizure morphology, all seizures not detected by the 5-feature detector were found to have significant recording gaps

(Figure 3). Clinical expert review (B.L.) indicates that these seizures, which were documented by patients, family members, or audio recordings, may also have been missed by expert readers if judged by iEEG recordings alone. Intermittent data loss from recording failure is a well-documented limitation of continuous iEEG analysis<sup>19,36,52,53</sup>. Improved device hardware, with improved battery life and data transmission reliability to minimize recording gaps, is required in order to reliably detect these seizures.

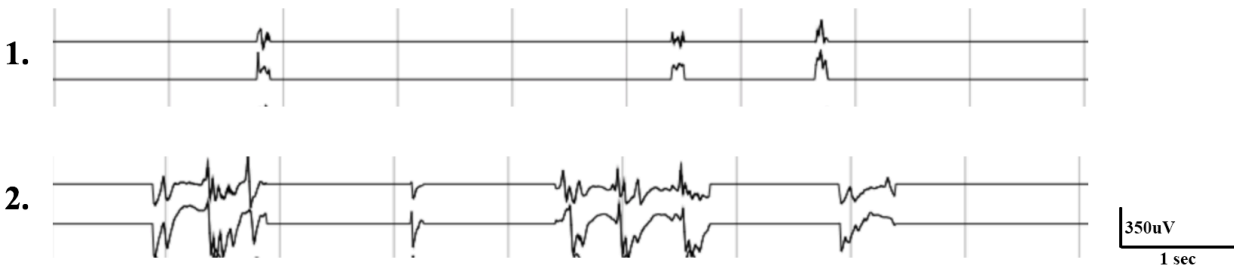


**Figure 3.** Examples of seizures undetected by the gating algorithm. The above two iEEG clips were recorded during patient-reported seizures and show significant data gaps because of failure of data transmission between implanted device and external NeuroVista patient assistant device. Example 1 shows only brief fragments (~0.2 sec) of iEEG that are difficult to classify electrographically on visual review. Example 2 shows iEEG fragments likely consistent with an electrographic seizure discharge on expert visual review. Neither example was detected by the gating algorithm due to recording gaps and therefore not transmitted to the cloud for analysis. Seizure activity was not detected for a sufficient length of time to trigger a detection.

There are also limitations with regard to the design of the gating algorithm itself. Feature selection through stepwise addition is not guaranteed to produce an optimal feature set, and may find local rather than global minima during training. In addition, the choice of a logistic regression classifier was made to ensure compatibility with device hardware. Logistic regression outperformed linear discriminate analysis (LDA), and performed as well or better than more complex methods (such as random forests<sup>54</sup> and support vector machines<sup>55</sup>) in the feature-limited environment.

Connectivity between medical devices and computer networks inherently introduces vulnerability to security breaches<sup>56,57</sup>. Attacks on networked medical devices capable of being reprogrammed wirelessly have potential to compromise data<sup>58</sup>, and to decrease device safety and efficacy<sup>59</sup>. As medical data is increasingly stored and analyzed remotely, new systemic metrics for data protection and encryption are being developed<sup>56,60–62</sup>. Proactive coordinated efforts between health care organizations, device manufacturers, and governing bodies are essential to understand and adapt to cybersecurity vulnerabilities already present in networked medical devices, and to embed protection into device design and manufacturing<sup>56</sup>.

This strategy of coupling local computation with cloud-based analysis can be generalized to other medical device applications. By using on-device algorithms for data reduction, we are able to leverage cloud computing resources when needed and operate within the hardware restrictions of implanted devices. This analytical structure allows for a shorter algorithm development cycle, as machine learning algorithms are remotely written and managed, and could be pushed into clinical care via centralized updates rather than local changes.

## **Conclusion**

In this study we demonstrate a novel framework for implementing computationally intensive algorithms on data recorded from an implanted neurodevice. While clinical studies are needed to confirm the efficacy of this paradigm *in vivo*, this study shows the feasibility and illustrates the potential benefits of such an approach. By using telemetry to access cloud-based computational resources, the next generation of neuro-implantable devices will leverage sophisticated algorithms that may greatly improve device performance and patient outcomes.

## Acknowledgements

This research was supported by the National Institutes of Health (NIH) (UH2/UH3-NS095495-01, R01NS092882-03, 1K01ES025436-01), the Mirowski Family Foundation, the Ashton Fellowship at the University of Pennsylvania, the Mayo Clinic Discovery Translation Grant, contributions from Neil and Barbara Smit, and institutional resources for research by Czech Technical University in Prague, Czech Republic. The International Epilepsy Electrophysiology (IEEG) Portal is funded by the NIH (5-U24-NS-063930-05). Dr. Brian Litt has licensed technology to NeuroPace, Inc. through the University of Pennsylvania, and is a founder of Blackfynn, Inc. Timothy Denison is an employee of Medtronic.

## References

1. Khan, W., Muntimadugu, E., Jaffe, M. & Domb, A. J. in 33–59 (2014). doi:10.1007/978-1-4614-9434-8\_2
2. Meng, E., Sheybani, R., Langer, R. & Langer, R. Insight: implantable medical devices. *Lab Chip* **14**, 3233 (2014).
3. Sun, F. T. & Morrell, M. J. Closed-loop Neurostimulation: The Clinical Experience. *Neurotherapeutics* **11**, 553–563 (2014).
4. Bergey, G. K. *et al.* Long-term treatment with responsive brain stimulation in adults with refractory partial seizures. *Neurology* **84**, 810–817 (2015).
5. Heck, C. N. *et al.* Two-year seizure reduction in adults with medically intractable partial onset epilepsy treated with responsive neurostimulation: Final results of the RNS System Pivotal trial. *Epilepsia* **55**, 432–441 (2014).
6. Denison, T., Morris, M. & Sun, F. Building a bionic nervous system. *IEEE Spectr.* **52**, 32–39 (2015).
7. Baldassano, S. N. *et al.* Crowdsourcing seizure detection: algorithm development and validation on human implanted device recordings. *Brain* **140**, 1680–1691 (2017).
8. Fisher, R. *et al.* Electrical stimulation of the anterior nucleus of thalamus for treatment of refractory epilepsy. *Epilepsia* **51**, 899–908 (2010).
9. Morrell, M. J. Responsive cortical stimulation for the treatment of medically intractable partial epilepsy. *Neurology* **77**, 1295–304 (2011).
10. Han, C.-L. *et al.* Electrical stimulation of hippocampus for the treatment of refractory temporal lobe epilepsy. *Brain Res. Bull.* **109**, 13–21 (2014).
11. Geller, E. B. *et al.* Brain-responsive neurostimulation in patients with medically intractable mesial temporal lobe epilepsy. *Epilepsia* **58**, 994–1004 (2017).
12. Nair, D. & Morrell, M. Long-term safety and efficacy of responsive brain stimulation in adults with medically intractable partial onset seizures (S21.004). *Neurology* **88**, (2017).
13. Kwan, P. & Brodie, M. J. Early identification of refractory epilepsy. *N. Engl. J. Med.* **342**, 314–9 (2000).

14. Ramgopal, S. *et al.* Seizure detection, seizure prediction, and closed-loop warning systems in epilepsy. *Epilepsy Behav.* **37**, 291–307 (2014).
15. Fountas, K. N. *et al.* Implantation of a closed-loop stimulation in the management of medically refractory focal epilepsy: a technical note. *Stereotact. Funct. Neurosurg.* **83**, 153–8 (2005).
16. Sun, F. T., Morrell, M. J. & Wharen, R. E. Responsive cortical stimulation for the treatment of epilepsy. *Neurotherapeutics* **5**, 68–74 (2008).
17. Morrell, M. Brain stimulation for epilepsy: can scheduled or responsive neurostimulation stop seizures? *Curr. Opin. Neurol.* **19**, 164–168 (2006).
18. Tzallas, A. T. *et al.* Automated epileptic seizure detection methods: a review study. *INTECH Open Access Publ.* (2012).
19. Brinkmann, B. H. *et al.* Forecasting Seizures Using Intracranial EEG Measures and SVM in Naturally Occurring Canine Epilepsy. *PLoS One* **10**, e0133900 (2015).
20. Kremen, V. *et al.* Behavioral state classification in epileptic brain using intracranial electrophysiology. *J. Neural Eng.* **14**, 026001 (2017).
21. Esteller, R., Echauz, J., Tcheng, T., Litt, B. & Pless, B. Line length: an efficient feature for seizure onset detection. in *2001 Conference Proceedings of the 23rd Annual International Conference of the IEEE Engineering in Medicine and Biology Society* **2**, 1707–1710 (IEEE, 2001).
22. Gotman, J. Automatic recognition of epileptic seizures in the EEG. *Electroencephalogr. Clin. Neurophysiol.* **54**, 530–540 (1982).
23. Echauz, J. *et al.* Long Term Validation of Detection Algorithms Suitable for an Implantable Device. *Epilepsia*, vol. 42, no suppl. 7 35–36 (2001). at  
<file:///Users/stevenbaldassano/Downloads/AES2001posterWsignif.pdf>
24. Herron, J., Denison, T. & Chizeck, H. J. Closed-loop DBS with movement intention. in *2015 7th International IEEE/EMBS Conference on Neural Engineering (NER)* 844–847 (IEEE, 2015). doi:10.1109/NER.2015.7146755
25. Ryapolova-Webb, E. *et al.* Chronic cortical and electromyographic recordings from a fully implantable device: preclinical experience in a nonhuman primate. *J. Neural Eng.* **11**, 016009 (2014).
26. Xanthopoulos, P., Pardalos, P. M. & Trafalis, T. B. in 27–33 (Springer, New York, NY, 2013). doi:10.1007/978-1-4419-9878-1\_4
27. Lundstrom, B. N. *et al.* Chronic Subthreshold Cortical Stimulation to Treat Focal Epilepsy. *JAMA Neurol.* **73**, 1370 (2016).
28. Lundstrom, B. N., Worrell, G. A., Stead, M. & Van Gompel, J. J. Chronic subthreshold cortical stimulation: a therapeutic and potentially restorative therapy for focal epilepsy. *Expert Rev. Neurother.* **17**, 661–666 (2017).
29. Morrell, M. J. & Halpern, C. Responsive Direct Brain Stimulation for Epilepsy. *Neurosurg. Clin. N. Am.* **27**, 111–121 (2016).
30. Fisher, R. S. & Velasco, A. L. Electrical brain stimulation for epilepsy. *Nat. Rev. Neurol.* **10**, 261–270 (2014).
31. Panescu, D. Emerging Technologies [wireless communication systems for implantable medical devices]. *IEEE Eng. Med. Biol. Mag.* **27**, 96–101 (2008).
32. Kiourti, A., Psathas, K. A. & Nikita, K. S. Implantable and ingestible medical devices with wireless telemetry functionalities: A review of current status and challenges. *Bioelectromagnetics* **35**, 1–15 (2014).
33. Yazdandoost, K. Y. & Kohno, R. Wireless Communications for Body Implanted Medical Device. in *2007 Asia-Pacific Microwave Conference* 1–4 (IEEE, 2007). doi:10.1109/APMC.2007.4554534
34. Bourget, D. *et al.* An implantable, rechargeable neuromodulation research tool using a distributed interface and algorithm architecture. in *2015 7th International IEEE/EMBS Conference on Neural Engineering (NER)* 61–65 (IEEE, 2015). doi:10.1109/NER.2015.7146560
35. Kremen, V. *et al.* Continuous active probing and modulation of neural networks with a wireless implantable system. in *2017 IEEE Biomedical Circuits and Systems Conference (BioCAS)* 1–4

- (IEEE, 2017). doi:10.1109/BIOCAS.2017.8325195
36. Cook, M. J. *et al.* Prediction of seizure likelihood with a long-term, implanted seizure advisory system in patients with drug-resistant epilepsy: a first-in-man study. *Lancet Neurol.* **12**, 563–571 (2013).
  37. Litt, B. *et al.* Epileptic Seizures May Begin Hours in Advance of Clinical Onset: A Report of Five Patients. *Neuron* **30**, 51–64 (2001).
  38. Kramer, M. A. *et al.* Coalescence and fragmentation of cortical networks during focal seizures. *J. Neurosci.* **30**, 10076–85 (2010).
  39. Khambhati, A. N. *et al.* Dynamic Network Drivers of Seizure Generation, Propagation and Termination in Human Neocortical Epilepsy. *PLOS Comput. Biol.* **11**, e1004608 (2015).
  40. Hocking, R. R. A Biometrics Invited Paper. The Analysis and Selection of Variables in Linear Regression. *Biometrics* **32**, 1 (1976).
  41. Quesney, L. F. Intracranial EEG investigation in neocortical epilepsy. *Adv. Neurol.* **84**, 253–74 (2000).
  42. Schiller, Y., Cascino, G. D., Busacker, N. E. & Sharbrough, F. W. Characterization and Comparison of Local Onset and Remote Propagated Electrographic Seizures Recorded with Intracranial Electrodes. *Epilepsia* **39**, 380–388 (1998).
  43. Quesney, L. F., Constain, M., Rasmussen, T., Olivier, A. & Palmini, A. Presurgical EEG investigation in frontal lobe epilepsy. *Epilepsy Res. Suppl.* **5**, 55–69 (1992).
  44. Worrell, G. A. *et al.* High-frequency oscillations and seizure generation in neocortical epilepsy. *Brain* **127**, 1496–1506 (2004).
  45. Ung, H. *et al.* Intracranial EEG fluctuates over months after implanting electrodes in human brain. *J. Neural Eng.* **14**, 056011 (2017).
  46. Huang, J. *et al.* A close examination of performance and power characteristics of 4G LTE networks. in *Proceedings of the 10th international conference on Mobile systems, applications, and services - MobiSys '12* 225 (ACM Press, 2012). doi:10.1145/2307636.2307658
  47. Bergland, G. Fast Fourier transform hardware implementations--An overview. *IEEE Trans. Audio Electroacoust.* **17**, 104–108 (1969).
  48. Davies, P. J. & Bohorquez, J. Design of a Portable Wireless EEG System Using a Fully Integrated Analog Front End. in *2013 29th Southern Biomedical Engineering Conference* 63–64 (IEEE, 2013). doi:10.1109/SBEC.2013.40
  49. Yu, R. *et al.* Smart healthcare: Cloud-enabled body sensor networks. in *2017 IEEE 14th International Conference on Wearable and Implantable Body Sensor Networks (BSN)* 99–102 (IEEE, 2017). doi:10.1109/BSN.2017.7936017
  50. Parastarfeizabadi, M. & Kouzani, A. Z. Advances in closed-loop deep brain stimulation devices. *J. Neuroeng. Rehabil.* **14**, 79 (2017).
  51. Xu, Z.-H. *et al.* Therapeutic time window of low-frequency stimulation at entorhinal cortex for amygdaloid-kindling seizures in rats. *Epilepsia* **51**, 1861–1864 (2010).
  52. Schelter, B., Timmer, J. & Schulze-Bonhage, A. *Seizure Prediction in Epilepsy: From Basic Mechanisms to Clinical Applications*. (Wiley-VCH, 2008).
  53. Litt, B. *et al.* Epileptic Seizures May Begin Hours in Advance of Clinical Onset: A Report of Five Patients. *Neuron* **30**, 51–64 (2001).
  54. Hastie, T., Tibshirani, R. & Friedman, J. *The Elements of Statistical Learning*. (Springer New York, 2009). doi:10.1007/978-0-387-84858-7
  55. Hearst, M. A., Dumais, S. T., Osuna, E., Platt, J. & Scholkopf, B. Support vector machines. *IEEE Intell. Syst. their Appl.* **13**, 18–28 (1998).
  56. Williams, P. A. & Woodward, A. J. Cybersecurity vulnerabilities in medical devices: a complex environment and multifaceted problem. *Med. Devices (Auckl)*. **8**, 305–16 (2015).
  57. *Networked medical device cybersecurity and patient safety: Perspectives of health care information security executives*. (2013).
  58. Li, M., Lou, W. & Ren, K. Data security and privacy in wireless body area networks. *IEEE Wirel.*

- Commun.* **17**, 51–58 (2010).
59. Halperin, D. *et al.* Pacemakers and Implantable Cardiac Defibrillators: Software Radio Attacks and Zero-Power Defenses. in *2008 IEEE Symposium on Security and Privacy (sp 2008)* 129–142 (IEEE, 2008). doi:10.1109/SP.2008.31
  60. Meingast, M., Roosta, T. & Sastry, S. Security and Privacy Issues with Health Care Information Technology. in *2006 International Conference of the IEEE Engineering in Medicine and Biology Society* 5453–5458 (IEEE, 2006). doi:10.1109/IEMBS.2006.260060
  61. Abbas, A. & Khan, S. U. A Review on the State-of-the-Art Privacy-Preserving Approaches in the e-Health Clouds. *IEEE J. Biomed. Heal. Informatics* **18**, 1431–1441 (2014).
  62. *Postmarket Management of Cybersecurity in Medical Devices: Guidance for Industry and Food and Drug Administration Staff.* (2016).